Effect of the ultrasonic emitter on the distortion performance of the parametric array loudspeaker

Chuang Shi[a,*], Yoshinobu Kajikawa[a]

[a]*Department of Electrical and Electronic Engineering, Kansai University, Osaka, Japan*

Abstract

The parametric array loudspeaker (PAL) is a type of directional loudspeaker that utilizes the nonlinear acoustic effect to create the audible sound in an ultrasonic beam. Due to this unusual sound principle, it is inevitable that nonlinear distortion is incurred in the sound transmission of the PAL. Numerous modulation methods aiming to reduce the nonlinear distortion have been developed on the basis of the Berktay's far-field solution, but they often perform in an unexpected manner. The degraded practical performance has been credited to the inaccuracy of the Berktay's far-field solution. In this paper, we demonstrate the effect of the ultrasonic emitter on the distortion performance of the PAL and suggest that the Berktay's far-field solution remains to be a good model equation.

Keywords: Parametric array loudspeaker, Ultrasonic emitter, Frequency response, Berktay's far-field solution, Merklinger's far-field solution

*Corresponding Author's Email: r148005@kansai-u.ac.jp

1. Introduction

The PAL is able to transmit a narrow sound beam in air from a small sized ultrasonic emitter [1, 2]. This ability is resultant from the nonlinear acoustic effect of an ultrasonic beam that consists of two frequencies, whereby the difference frequency is generated as one of the extraneous frequencies [3]. The directivity of the difference frequency is described by an end-fire array, which gives a similarly narrow beamwidth as the ultrasonic beam [4, 5]. The PAL is readily adopted in various sound applications, such as active noise control [6], audio projection [7], human-machine interface [8], and even in an increasing number of contemporary art works [9, 10].

Figure 1 shows the block diagram of the PAL. The audio input is modulated on an ultrasonic carrier. The modulated input becomes an ultrasonic signal, which is then amplified to drive the ultrasonic emitter. The nonlinear acoustic effect in air distorts the waveform transmitted from the ultrasonic emitter and thus creates the audible sound. It is noteworthy that as compared to the ultrasound level, the audible sound pressure level is relatively weak. The ultrasound level must be controlled under safety regulations [11].

The Khokhlov-Zabolotskaya-Kuznetsov (KZK) equation describes the combined nonlinear acoustic effect of absorption, diffraction, and nonlinearity. It is one of the most efficient model equations of the PAL, but there is no analytical solution to the KZK equation [12]. Alternatively, Berktay provided a simple model equation for the far-field on-axis case, which states that the audible sound pressure level is proportional to the second derivative of the squared envelope of the modulated input [13].

Modulation methods have been developed for the PAL. The double side-

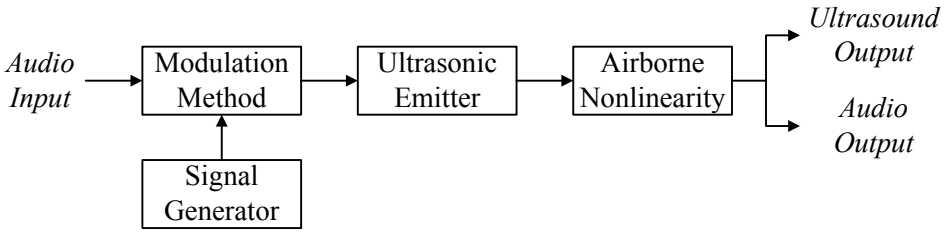

Figure 1: Block diagram of the PAL.

band (DSB) modulation method was carried out in the world first PAL [1]. Based on the Berktay's far-field solution, the second harmonic distortion level of the DSB modulation method is proportional to the modulation index and the frequency response possesses a slope of 12 dB per octave as a result of the second derivative. Kamakura *et al.* [14] proposed the square root (SRT) modulation method that provided an inverse system to the Berktay's far-field solution. Further development of the SRT modulation method preprocessed the audio input by a double integral to offset the 12 dB per octave slope [15].

There is another trend of the modulation method. The single sideband (SSB) modulation method, which is a type of quadrature modulation method, has been studied since the early days of the PAL [16]. The SSB modulation method includes a quadrature path to cancel the nonlinear distortion. The DSB and SSB modulation methods have individual advantages. So far, there have been two hybrid modulation methods combining the DSB and SSB modulation methods. The weighted DSB modulation method makes use of the relative high audible sound pressure level of the DSB modulation method to enhance the SSB modulation method at the low frequency band [17], while the asymmetrical amplitude modulation (AAM) method is a part of the audio bandwidth extension technique for the PAL [18, 19].

Similar to the SSB modulation method, the modified amplitude modulation (MAM) methods are quadrature modulation methods too [20]. The quadrature path in the SSB modulation method is often implemented by the Hilbert filter, while quadrature paths in the MAM methods are calculated by polynomial equations. The MAM methods using higher order polynomial equations are developed to achieve better distortion performance. Previous studies of the MAM methods provide simulation results only [21]. There is a lack of experiment validation of the MAM methods [22, 23].

Therefore, this paper aims to highlight the effect of the ultrasonic emitter on the distortion performance of the PAL. Modulation methods are comparatively evaluated under the same condition by simulations and measurements. The Berktay's far-field solution and the Merklinger's far-field solution are adopted as the model equations in the simulation [13, 24]. It is found that the discrepancy between the theoretical and measurement results is greater for the more sophisticated modulation method, if the frequency response of the ultrasonic emitter is ignored.

2. Model Equations

2.1. Berktay's Far-field Solution

To derive the Berktay's far-field solution, the primary sound pressure level is assumed in the one-dimension form of

$$p_1 = P_0 E\left(t\right) \exp\left(-\alpha_0 z\right) \cos\left(\omega_0 t\right), \tag{1}$$

where P_0, α_0, and ω_0 are initial pressure level, attenuation rate, angular frequency of the ultrasonic carrier, respectively; t is the retarded time; z is

the on-axis coordinate; and $E(t)$ is the envelope of the modulated input, which is assumed to have an unit amplitude.

Subsequently, the audible sound source strength density is written as

$$q_d = \frac{\beta P_0^2}{\rho_0^2 c_0^4} \exp\left(-2\alpha_0 z\right) \frac{\partial}{\partial t}\left[\frac{E^2(t)}{2}\right], \tag{2}$$

where β is the nonlinear coefficient; ρ_0 is the density of air; and c_0 is the speed of sound in air.

The audible sound pressure level is thus calculated by

$$p_d(x) = \frac{\rho_0 a^2}{4x} \int_0^{+\infty} \frac{\partial q_d}{\partial t} dz = \frac{\beta P_0^2 a^2}{16\rho_0 c_0^4 \alpha_0 x} \frac{\partial^2}{\partial t^2} E^2(t), \tag{3}$$

where x is the observation point and a is the radius of the ultrasonic emitter.

2.2. Merklinger's Far-field Solution

In Berktay's derivation, the primary sound pressure level is assumed to decrease with distance by the thermoviscous absorption effect only. Merklinger extended the Berktay's far-field solution to include the nonlinear absorption effect [25]. The energy transfered from the primary sound to the second harmonic of the primary sound, which is much greater than the energy transfered from the primary sound to the audible sound, attenuates the primary sound pressure level to become

$$p_1 = \frac{P_0 E(t) \exp\left(-\alpha_0 z\right)}{\sqrt{1 + \Gamma^2 E^2(t) \left[1 - \exp\left(-2\alpha_0 z\right)\right]^2 / 16}} \cos\left(\omega_0 t\right), \tag{4}$$

where Γ is called the Gol'dberg number [26] and defined as

$$\Gamma = \frac{\beta P_0 \omega_0}{\rho_0 c_0^3 \alpha_0}. \tag{5}$$

If a modified envelope function is correspondingly defined as

$$E'(t) = \frac{E(t)}{\sqrt{1 + \Gamma^2 E^2(t) \left[1 - \exp\left(-2\alpha_0 z\right)\right]^2 / 16}}, \tag{6}$$

(2) and the integral in (3) are still valid to calculate the audible sound pressure level. Therefore, the Merklinger's far-field solution is given by

$$p_d(x) = \frac{P_0 a^2}{4\omega_0 c_0 x} \frac{\partial^2}{\partial t^2} \{E(t) \tan^{-1}\left[\Gamma E(t)/4\right]\}. \tag{7}$$

When $\Gamma E(t)/4$ is small, substituting $\tan^{-1}\left[\Gamma E(t)/4\right] \approx \Gamma E(t)/4$ into (7) yields the Berktay's far-field solution. When $\Gamma E(t)/4$ is large, $\tan^{-1}\left[\Gamma E(t)/4\right]$ is approximated by $\mathrm{sgn}\left[E(t)\right]\pi/2$. This makes (7) simplified to a concise expression as

$$p_d(x) = \frac{P_0 \pi a^2}{8\omega_0 c_0 x} \frac{\partial^2}{\partial t^2} |E(t)|. \tag{8}$$

Most of the PALs utilize the ultrasonic carrier at 40 kHz. When the ultrasonic carrier is transmitted at the initial pressure level of 110 dB, the Gol'dberg number in the general room condition approximates 0.4 [26]. Therefore, the Berktay's far-field solution is valid and the second order nonlinearity $E^2(t)$ determines the audible sound pressure level. However, when the initial pressure level increases to 130 dB, the Gol'dberg number is proportional to the initial pressure level and becomes 4.0. The audible sound pressure level is associated with $E(t) \tan^{-1} E(t)$, as described by the Merklinger's far-field solution. Since the safety of using ultrasound in public is an important concern, the initial pressure level of the ultrasonic carrier is more likely to be set close to 110 dB rather than 130 dB.

3. Modulation methods

3.1. DSB Modulation Method

The DSB modulation method is the first modulation method applied in the PAL [1]. The envelope of the DSB modulation method is written as

$$E^{DSB}(t) = 1 + mx(t), \tag{9}$$

where m is the modulation index and $x(t)$ is the audio input. The disadvantage of the DSB modulation method has been well known. Substituting (9) into the Berktay's far-field solution yields the audible sound pressure level as

$$p_d^{DSB} \propto \frac{\partial^2}{\partial t^2}\left[2mx(t) + m^2x^2(t)\right]. \tag{10}$$

The second harmonic distortion level of the DSB modulation method is credited to the second term in the bracket.

The distortion performance of the DSB modulation method is improved when the Gol'dberg number is increased. If the Merklinger's far-field solution becomes the dominating model equation, substituting (9) into (8) yields the audible sound pressure level as

$$p_d^{DSB} \propto \frac{\partial^2}{\partial t^2} mx(t). \tag{11}$$

In this case, the DSB modulation method has the ideal linear response.

3.2. SRT Modulation Method

The SRT modulation method is an inverse system to the Berktay's far-field solution [14]. The envelope of the SRT method is written as

$$E^{SRT}(t) = \sqrt{1 + mx(t)}. \tag{12}$$

Similarly, the audible sound pressure level of the SRT modulation method is given by

$$p_d^{SRT} \propto \frac{\partial^2}{\partial t^2} mx\left(t\right). \tag{13}$$

It is observed in (13) that the SRT modulation method is able to completely eliminate the nonlinear distortion. However, because of the square root operation, the SRT modulation method necessitates an ideal ultrasonic emitter with an infinite bandwidth.

The truncated SRT modulation method is useful for us to understand the SRT modulation method analytically. The Taylor series expansion of (12) is written as

$$E^{SRTq}\left(t\right) = \sum_{i=0}^{q} \frac{\left(2i\right)!}{\left(1-2i\right)\left(i!\right)^2\left(-4\right)^i} m^i x^i\left(t\right). \tag{14}$$

Taking $q = 2$ leads to the SRT2 modulation method, whose envelope function is written as

$$E^{SRT2}\left(t\right) = 1 + \frac{m}{2} x\left(t\right) - \frac{m^2}{8} x^2\left(t\right). \tag{15}$$

Substituting (15) into the Berktay's far-field solution yields the audible sound pressure level as

$$p_d^{SRT2} \propto \frac{\partial^2}{\partial t^2}\left[mx\left(t\right) - \frac{m^3}{8} x^3\left(t\right) + \frac{m^4}{64} x^4\left(t\right)\right]. \tag{16}$$

Eq. (16) implies that the SRT modulation method is essentially an approach to shift the nonlinear distortion to higher order, *i.e.* the third and forth order terms in (16), by introducing lower order harmonics of the audio input, *i.e.* the second order term in (15).

Moreover, when the Gol'dberg number is large, the audible sound pressure level of the SRT2 modulation method becomes

$$p_d^{SRT2} \propto \frac{\partial^2}{\partial t^2}\left[\frac{m}{2} x\left(t\right) - \frac{m^2}{8} x^2\left(t\right)\right]. \tag{17}$$

Therefore, the distortion performance of the SRT modulation method is not much affected by the Gol'dberg number, when the modulation index is small. When the modulation index is large, increasing the Gol'dberg number significantly worsens the distortion performance of the SRT modulation method.

3.3. Modified Amplitude Modulation Methods

Although the MAM methods are quadrature modulation methods in form, they adopt a similar idea of the SRT modulation method. The MAM methods introduce lower even order harmonics of the audio input to shift the nonlinear distortion to higher even order. The modulated input of the root MAM method is written as

$$p_1^{MAM}(t) = E^{DSB}\cos(\omega_0 t) + Q^{MAM}(t)\sin(\omega_0 t), \tag{18}$$

where the quadrature term is given by

$$Q^{MAM}(t) = \sqrt{1 - m^2 x^2(t)}. \tag{19}$$

Therefore, the envelope of the root MAM method is written as

$$E^{MAM}(t) = \sqrt{\left[E^{DSB}(t)\right]^2 + \left[Q^{MAM}(t)\right]^2} = \sqrt{2 + 2mx(t)}. \tag{20}$$

The root MAM method has the same envelope as the SRT modulation method. However, as the quadrature term includes the square root operation, the root MAM method also necessitates an ideal ultrasonic emitter with an infinite bandwidth. Therefore, the MAMq methods have been proposed to take the truncated Taylor series expansion of (19) as

$$Q^{MAMq}(t) = \sum_{i=0}^{q} \frac{(2i)!}{(1-2i)(i!)^2 4^i} m^{2i} x^{2i}(t). \tag{21}$$

Hence, the quadrature terms of the MAM1 and MAM2 methods are written as

$$Q^{MAM1}(t) = 1 - \frac{m^2}{2}x^2(t) \tag{22}$$

and

$$Q^{MAM2}(t) = 1 - \frac{m^2}{2}x^2(t) - \frac{m^4}{8}x^4(t). \tag{23}$$

It is also noteworthy that the MAM1 method requires the same bandwidth of the ultrasonic emitter as the SRT2 modulation method, while the MAM2 method requires the bandwidth to be doubled.

Applying the Berktay's far-field solution yields the audible sound pressure levels, which are given by

$$p_d^{MAM1} \propto \frac{\partial^2}{\partial t^2}\left[2mx(t) + \frac{m^4}{4}x^4(t)\right] \tag{24}$$

and

$$p_d^{MAM2} \propto \frac{\partial^2}{\partial t^2}\left[2mx(t) + \frac{m^6}{8}x^6(t) + \frac{m^8}{64}x^8(t)\right]. \tag{25}$$

The MAM methods result in higher order nonlinear distortion than the truncated SRT methods requiring the same bandwidth.

When the Gol'dberg number is relatively large, the MAM methods become less dependent on the truncation order and lead to more distortion than the SRT modulation method, as shown by the audible sound pressure levels obtained from (8):

$$p_d^{MAM1} \propto \frac{\partial^2}{\partial t^2}\left[\sqrt{2 + 2mx(t) + \frac{m^4}{4}x^4(t)}\right] \tag{26}$$

and

$$p_d^{MAM2} \propto \frac{\partial^2}{\partial t^2}\left[\sqrt{2 + 2mx(t) + \frac{m^6}{8}x^6(t) + \frac{m^8}{64}x^8(t)}\right]. \tag{27}$$

4. Results

4.1. Theoretical Results

The theoretical results are presented first. An ultrasonic carrier at 40 kHz and a sine sweep from 0.5 kHz to 8 kHz are generated for the theoretical simulation. The sine sweep is modulated on the ultrasonic carrier by the aforementioned preprocessing methods at different modulation indexes from 0.1 to 1.0. The second derivative is implemented by two digital differential filters. Both the Berktay's far-field solution and the Merklinger's far-field solution are adopted. The Gol'dberg numbers are subsequently set to 0.4 and 4.0 for comparison. The total harmonic distortion (THD) level is calculated by the root mean squared (RMS) amplitude of the audible harmonics divided by the amplitude of the fundamental frequency. The calculated THD levels at different fundamental frequencies are averaged and plotted in Fig. 2.

The results obtained from the Berktay's far-field solution and the Merklinger's far-field solution when $\Gamma = 0.4$ have no notable difference. The SRT modulation method shows the perfect THD performance, while the DSB modulation method leads to the worst THD performance. The MAM methods are able to adjust the THD performance by the truncation order. However, in Fig. 2(c), the THD performance of the DSB modulation method is improved as a result of the increased Gol'dberg number. The performance difference among the SRT and MAM modulation methods is reduced. If we rank the modulation methods by their THD performance, the sequence of the MAM methods is interestingly reversed in Fig. 2(c) as compared to Fig. 2(b). These observations agree with the analyses based on equations presented in the previous section.

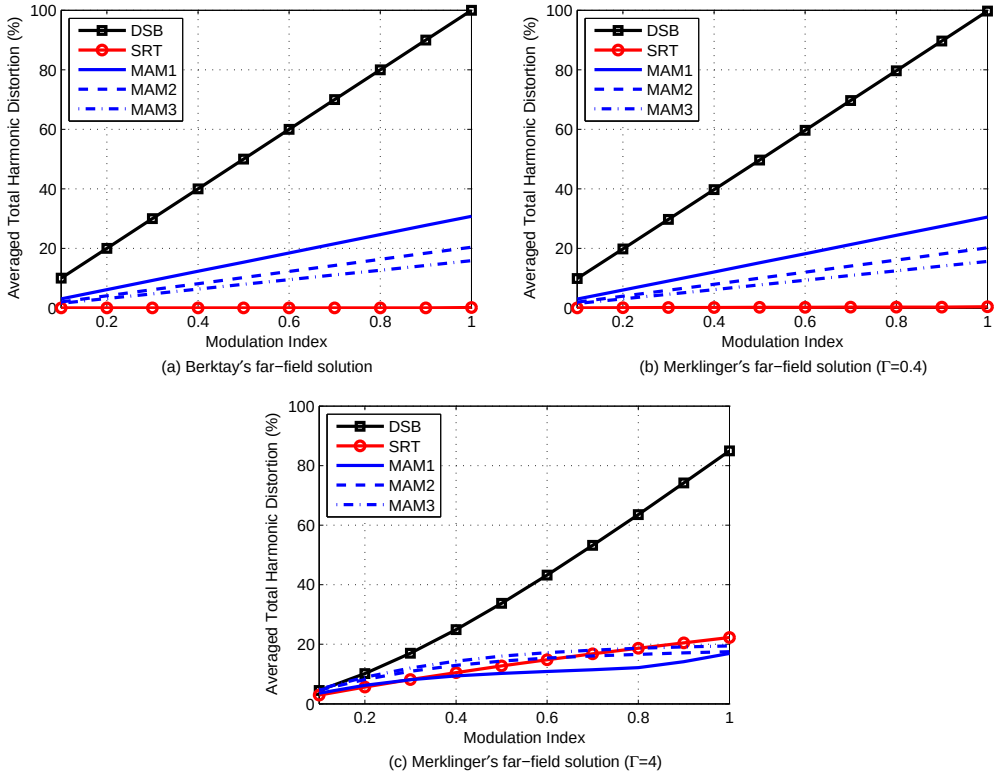

Figure 2: Theoretical averaged THD performance of a sine sweep from 0.5 kHz to 8 kHz.

In addition to the THD test, the intermodulation distortion (IMD) test is also carried out. Another sine tone at 1.7 kHz is generated. It is mixed with the sine sweep to provide the testing audio input. The amplitude ratio between the sine tone and the sine sweep is 4:1. The IMD level is calculated by the RMS amplitude of the audible intermodulation frequencies divided by the RMS amplitude of the fundamental frequencies. The averaged IMD levels are plotted in Fig. 3. In short, Fig. 3 reflects a scaled version of Fig. 2.

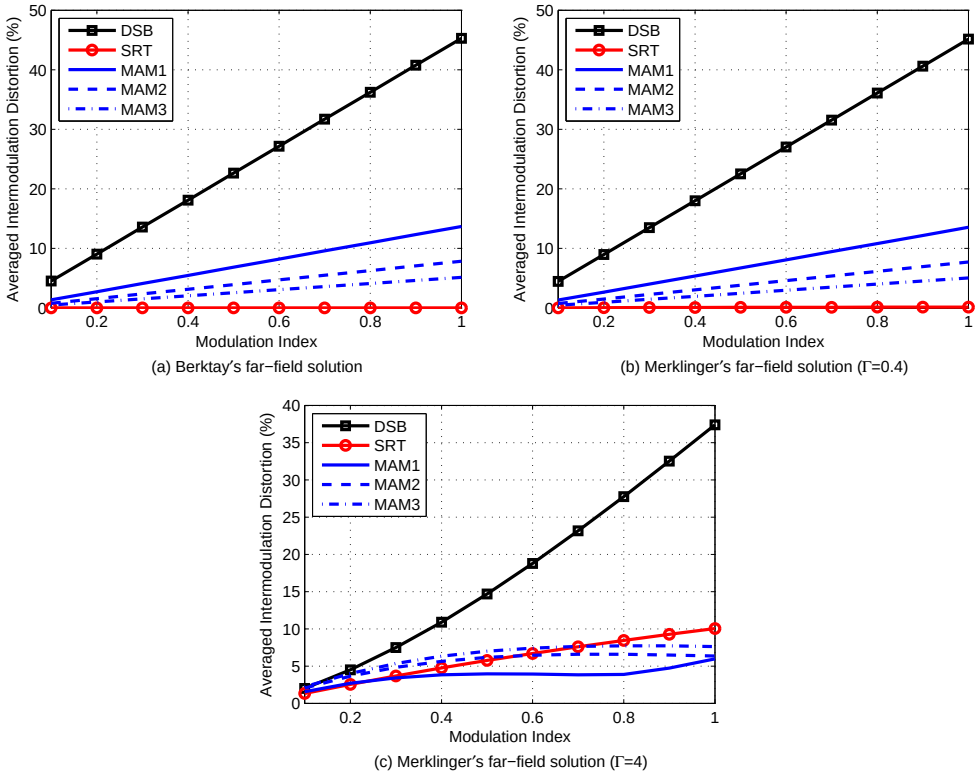

Figure 3: Theoretical averaged IMD performance of a sine sweep from 0.5 kHz to 8 kHz and a sine tone at 1.7 kHz.

4.2. Experiment Results

The experiment was carried out in a sound proof room ($2.9 \times 3.1 \times 2.1\ m^3$), where a B&K Type 4191L microphone and an ultrasonic emitter supplied by Mitsubishi Electronic Engineering Company were installed. The ultrasonic carrier and testing audio inputs were prepared in the same way as those in the simulation. The THD and IMD levels were measured at a distance of 300 cm from the ultrasonic emitter. Since the diameter of the ultrasonic emitter was 18 cm, this distance barely ensured the far-field condition of the measurement. The ultrasound level was limited at 110 dB for different modulation methods by (1) fixing the gain of the amplifier and (2) normalizing the digital signal before sending it to the digital-to-analog converter. Furthermore, the frequency response of the ultrasonic emitter was also measured between 50 cm and 300 cm with an interval of 50 cm. In this case, the gain of the amplifier was turned up to make the ultrasound level approaching 130 dB.

The measured frequency responses of the ultrasonic emitter are plotted in Fig. 4(a). It is noted that with an exception of the frequency response measured at 50 cm, the rest of measurement data are very similar in trend. Because within the very near field of the ultrasonic emitter, the pressure level may not decrease with the distance, we consider the frequency response measured at 50 cm as an outlier. The rest of measurement data are used to obtain an estimate of the frequency response of the ultrasonic emitter on its surface by the extrapolation method. The estimated frequency response is also plotted in Fig. 4(a). A finite impulse repose (FIR) filter with a memory size of 500 tapes is designed to fit the estimated frequency response from 20

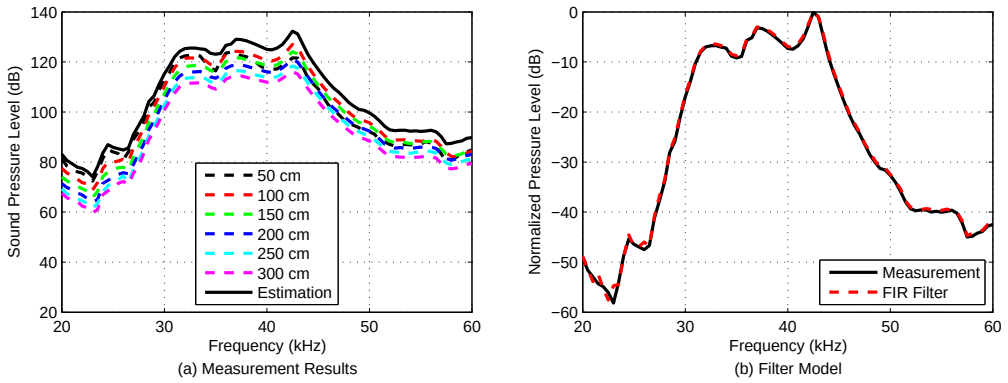

Figure 4: Measured and modeled frequency responses of the ultrasonic emitter for test.

kHz to 60 kHz, as shown in Fig. 4(b). This digital filter is later used to preprocess the modulated input before the model equations are applied in the simulation.

The simulated and measured THD levels are plotted in Fig. 5. Fig. 5(b) presents the closest results to Fig. 5(d), and Fig. 5(a) is in good agreement with the measurement results as well. These observations demonstrate that the Merklinger's far-field solution is more accurate, while the Berktay's far-field solution remains to be a good model equation. Furthermore, Fig. 5(c) provides a meaningful prediction when the Gol'dberg number is large. In this case, the DSB modulation method outperforms the SRT modulation method, while the performance of the MAM methods is not much affected.

The frequency response of the ultrasonic emitter exhibits a significant effect on the THD performance of modulation methods, based on the comparison between Figs. 2 and 5. Since the DSB modulation method is a relatively simple modulation method, the measured THD performance is still proportional to the modulation index. However, the measured THD performance of

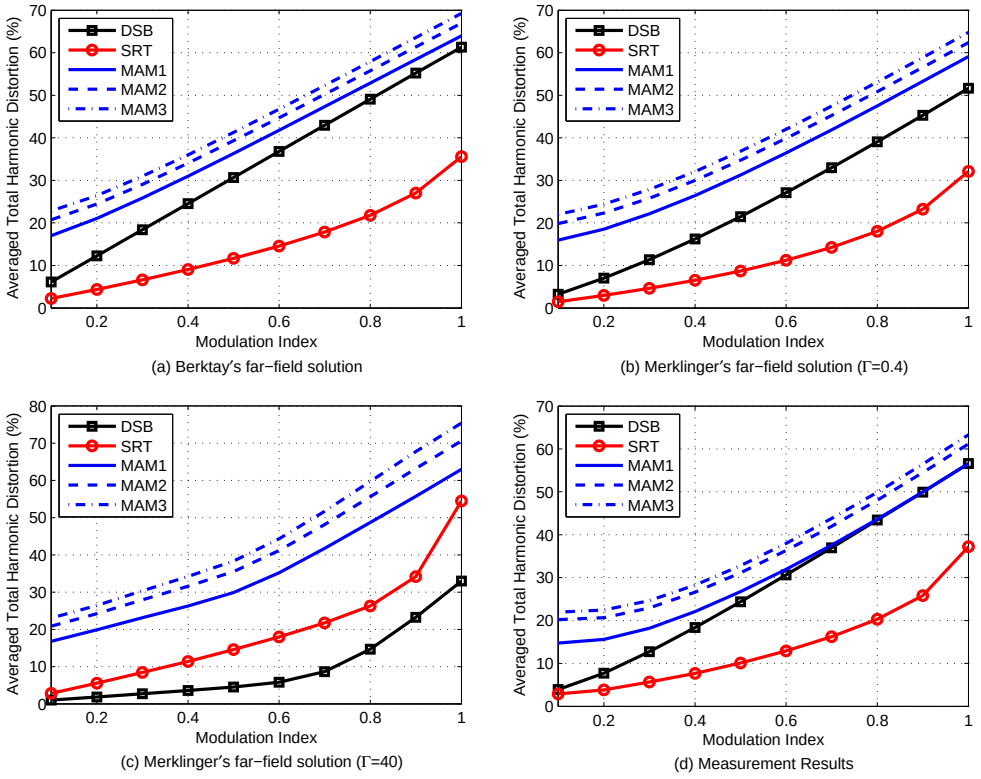

Figure 5: Simulated and measured averaged THD performance of a sine sweep from 0.5 kHz to 8 kHz.

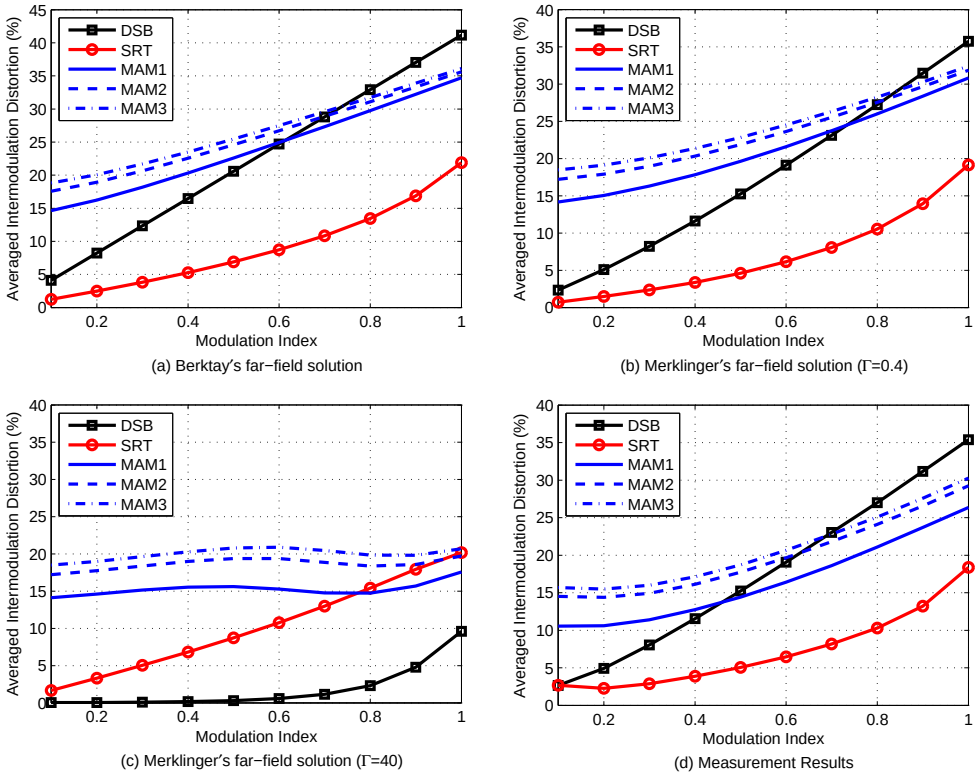

Figure 6: Simulated and measured averaged IMD performance of a sine sweep from 0.5 kHz to 8 kHz and a sine tone at 1.7 kHz.

the SRT modulation method possesses a quasi parabolic curve with respect to the modulation index. This is explained by the fact that the SRT2 method is the effective modulation method, due to the limited bandwidth of the ultrasonic emitter. For the same reason, the MAM methods result in notable second and third order distortion. The MAM methods behave similarly to a combination of the DSB and SRT modulation methods.

The simulated and measured IMD levels are plotted in Fig. 6. The subplots in Fig. 6 are almost scaled versions of the subplots in Fig. 5, except

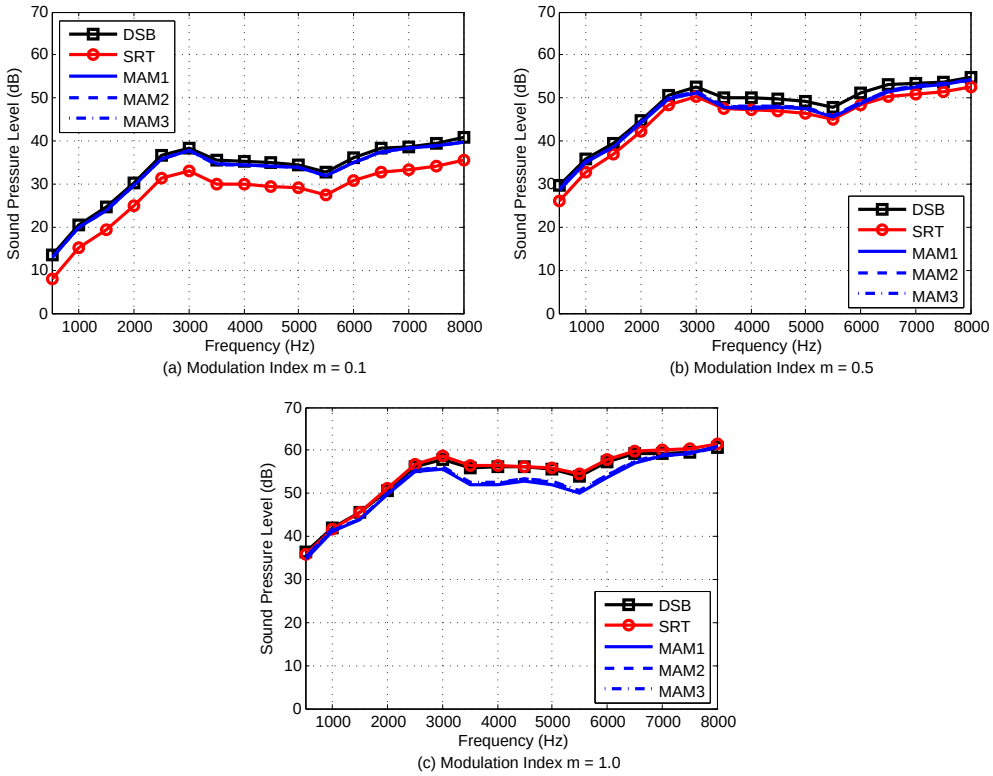

Figure 7: Measured frequency response from 0.5 kHz to 8 kHz.

for Fig. 6(c). Fig. 6 once again demonstrates that although the Merklinger's far-field solution is a more accurate model equation, the Berktay's far-field solution still provides good accuracy. The notable difference between Figs. 3 and 6 shows the effect of the ultrasonic emitter on the IMD performance of modulation methods. In Fig. 6(c), the DSB modulation method becomes the best modulation method, while the IMD performance of the SRT modulation method turns out to be proportional to the modulation index. This predicts the situation when the Gol'dberg number is so large that the ultrasound exposure might be dangerous to the listener.

Last but not least, the measured frequency responses of different modulation methods are plotted in Fig. 7 to validate the measured frequency responses of the ultrasonic emitter. The same methodology has been adopted by the inventors of the PAL [1]. In Fig. 4, there are three ripples, which are rarely observed in an ultrasonic emitter. The two peaks appearing at 37 kHz and 42.5 kHz can cause high audible sound pressure levels at 2.5 kHz and 3 kHz, which are confirmed in Fig. 7. Since there is a trough at 40.5 kHz in the frequency response of the ultrasonic emitter, the audible sound pressure level of the PAL is expected to be boosted at the low frequency band. Consequently, it is noted in Fig. 7 that the 12 dB per octave slope is improved to 10 dB per octave from 1 kHz to 2.5 kHz. Another trough in the frequency response of the ultrasonic emitter appears in between 45 kHz and 45.5 kHz. Therefore, a trough at 5.5 kHz is always observed in Fig. 7 regardless of the modulation method. In addition, the averaged audible sound pressure level of the PAL is monotonically associated with the modulation index, provided that the Gol'dberg number does not change.

5. Conclusions

This paper addresses a practical issue of the PAL on understanding discrepancies between the theoretical and measured distortion performance. Through theoretical derivations, simulations, and experiments, we have demonstrated that it is feasible to predict the distortion performance of the PAL by considering the frequency response of the ultrasonic emitter and using the Berktay's far-field solution. The Berktay's far-field solution remains to be a good model equation. But the Merlinger's far-field solution has demon-

strated better accuracy and ability to be applied in the situation when the Gol'dberg number is relatively large.

6. Acknowledgements

This work is supported by MEXT-Supported Program for the Strategic Research Foundation at Private University, 2013-2017. The first author would like to thank Professor Tomoo Kamakura for the informative discussions from time to time.

7. References

[1] M. Yoneyama, J. Fujimoto, Y. Kawamo, and S. Sasabe, "The audio spotlight: An application of nonlinear interaction of sound waves to a new type of loudspeaker design," *J. Acoust. Soc. Am.*, **73**, 1532–1536 (1983).

[2] W. S. Gan, J. Yang, and T. Kamakura, "A review of parametric acoustic array in air," *Applied Acoust.*, **73**, 1211–1219 (2012).

[3] A. L. Thuras, R. T. Jenkins, aud H. T. O'Neill, "Extraneous frequencies generated in air carrying intense sound waves," *J. Acoust. Soc. Amer.*, **6**, 173–180 (1935).

[4] P. J. Westervelt, "Parametric end-fire array," *J. Acoust. Soc. Amer.*, **32**, 934–935 (1960).

[5] P. J. Westervelt, "Parametric acoustic array," *J. Acoust. Soc. Amer.*, **35**, 535–537 (1963).

[6] B. Lam, W. S. Gan, and C. Shi, "Feasibility of a length-limited parametric source for active noise control applications," *Proc. 21st Int. Congr. Sound Vib.*, Beijing, China, 1–8 (2014).

[7] S. Takeoka and Y. Yamasaki, "Acoustic projector using directivity controllable parametric loudspeaker array," *Proc. 20th Int. Congr. Acoust.*, Sydney, Australia, 921-925 (2010).

[8] K. Nakadai and H. Tsujino, "Towards new human-humanoid communication Listening during speaking by using ultrasonic directional speaker," *Proc. IEEE Int. Conf. Robot. Autom.*, Barcelona, Spain, 1483–1488 (2005).

[9] K. Kimura, O. Hoshuyama, T. Tanikawa, and M. Hirose, "VITA: Visualization system for interaction with transmitted audio signals," *Proc. ACM SIGGRAPH*, Vancouver, Canada, Poster No. 54 (2011).

[10] M. Ueta, O. Hoshuyama, T. Narumi, T. Tanikawa, and M. Hirose, "JUKE Cylinder: a device to metamorphose hands to a musical instrument," *Proc. ACM SIGGRAPH*, Los Angeles, California, Poster No. 13 (2012).

[11] C. Shi and Y. Kajikawa, "Automatic gain control for parametric array loudspeakers," *Proc. 41th Int. Conf. Acoust. Speech Sig. Process.*, Shanghai, China, TBD (2016).

[12] Y. S. Lee, "Numerical solution of the KZK equation for pulsed finite amplitude sound beams in thermoviscous fluids," Doctor of Philosophy Dissertation, The University of Texas, Austin, United States, 1993.

[13] H. O. Berktay, "Possible exploitation of non-linear acoustics in underwater transmitting applications," *J. Sound Vib.* **2**, 435-461 (1965).

[14] T. Kamakura, M. Yoneyama, and K. Ikegaya, "Developments of parametric loudspeaker for practical use," *Proc. 10th Int. Symp. Nonlinear Acoust.*, Kobe, Japan, 147–150 (1984).

[15] T. D. Kite, J. T. Post, and M. F. Hamilton, "Parametric array in air distortion reduction by preprocessing," *J. Acoust. Soc. Am.* **103**, 2871 (1998).

[16] K. Aoki, T. Kamakura, and Y. Kumamoto, "Parametric loudspeaker: Characteristics of acoustic field and suitable modulation of carrier ultrasound," *Electron. Comm. Jpn* **74**, 76–82 (1991).

[17] D. Ikefuji, M. Nakayama, T. Nishiura, and Y. Yamashita, Weighted double sideband modulation toward high quality audible sound on parametric loudspeaker," *Proc. 38th Int. Conf. Acoust. Speech Sig. Process.*, Vancouver, Canada, 843–847 (2013).

[18] C. Shi and W. S. Gan, "A preprocessing method to increase high frequency response of a parametric loudspeaker," *Proc. 2013 APSIPA Annu. Summit Conf.*, Kaohsiung, Taiwan, 1–5 (2013).

[19] C. Shi, H. Mu, and W. S. Gan, "A psychoacoustical preprocessing technique for virtual bass enhancement of the parametric loudspeaker," *Proc. 38th Int. Conf. Acoust. Speech Sig. Process.*, Vancouver, Canada, 31–35 (2013).

[20] Y. H. Liew, "Signal processing techniques for sound reproduction in parametric arrays," Master Thesis, Nanyang Technological University, Singapore, 2002.

[21] E. L. Tan, P. Ji, and W. S. Gan, "On preprocessing techniques for bandlimited parametric loudspeakers," *Applied Acoust.*, **71**, 486–492 (2010).

[22] P. Ji, E. L. Tan, W. S. Gan, and J. Yang, "A comparative analysis of preprocessing methods for the parametric loudspeaker based on the Khokhlov-Zabolotskaya-Kuznetsov equation for speech reproduction," *IEEE Audio Speech Language Process.*, **19**, 937–946 (2011).

[23] C. Shi and Y. Kajikawa, "Evaluation of modified amplitude modulation methods in the parametric array loudspeaker," *IEICE Tech. Rep.*, **114**, 67–70 (2015).

[24] H. M. Merklinger, "Improved efficiency in the parametric transmitting array," *J. Acoust. Soc. Amer.*, **58**, 784–787 (1975).

[25] H. M. Merklinger, "Fundamental-frequency component of a finite-amplitude plane wave," *J. Acoust. Soc. Amer.*, **58**, 1760–1761 (1973).

[26] W. Kim and V. W. Sparrow, "Audio application of the parametric array: Implementation through a numerical model," *Proc. 113th Audio Eng. Soc. Conv.*, Los Angeles, California, 1–16 (2002).